



PAPER

View Article Online
View Journal | View IssueCite this: *Dalton Trans.*, 2025, **54**,
9359A water-soluble heterometallic iron(IV)–
ruthenium(IV) μ -nitrido porphyrin complex:
synthesis, structure and catalytic activity†Rain Ng, Wai-Man Cheung, Cheuk-Pui Leung, Chun Kit Au, Yat-Ming So,
Herman H.-Y. Sung, Wan Chan,* Ian D. Williams * and Wa-Hung Leung *

A heterometallic Fe(IV)–Ru(IV) nitrido complex bearing a water-soluble porphyrin ligand has been synthesized, and its redox and catalytic properties have been investigated. Treatment of $\text{Na}_4[\text{Fe}(\text{TPPS})(\text{H}_2\text{O})_2]$ ($[\text{TPPS}]^{4-}$ = *meso*-tetrakis(4-sulfonatophenyl)porphyrinate) with $[\text{Ru}(\text{N})(\text{LOEt})\text{Cl}_2]$ ($\text{LOEt}^- = [\text{Co}(\eta^5\text{-C}_5\text{H}_5)\{\text{P}(\text{O})(\text{OEt})_2\}_3]^-$) afforded the water-soluble μ -nitrido complex $\text{Na}_4[(\text{H}_2\text{O})(\text{TPPS})\text{Fe}(\mu\text{-N})\text{RuCl}_2(\text{LOEt})]$ ($\text{Na}_4[\mathbf{1}]$). Cation metathesis of $\text{Na}_4[\mathbf{1}]$ with $\text{Ph}_4\text{P}^+\text{Cl}^-$ gave $(\text{Ph}_4\text{P})_4[(\text{H}_2\text{O})(\text{TPPS})\text{Fe}(\mu\text{-N})\text{RuCl}_2(\text{LOEt})]$ ($(\text{Ph}_4\text{P})_4[\mathbf{1}]$), which has been characterized by single-crystal X-ray diffraction. The observed Ru–N(nitride) [1.701(5) Å] and Fe–N(nitride) [1.676(5) Å] distances and the Fe–N–Ru angle [171.4(3)°] of diamagnetic $[\mathbf{1}]^{4-}$ are indicative of the Fe(IV)=N= Ru(IV) bonding behavior. The cyclic voltammogram of $\text{Na}_4[\mathbf{1}]$ in 0.1 M HCl displayed reversible redox couples at +0.66 and +0.94 V versus a saturated calomel electrode, which are assigned metal-centred and porphyrin-based oxidations, respectively. Treatment of $\text{Na}_4[\mathbf{1}]$ with $\text{Ag}(\text{CF}_3\text{SO}_3)$ and PPh_3 resulted in the formation of $\text{Na}_3[(\text{H}_2\text{O})(\text{TPPS})\text{Fe}(\mu\text{-N})\text{Ru}(\text{LOEt})\text{Cl}_2(\text{Ag}(\text{PPh}_3))]$ ($\mathbf{2}$). $\text{Na}_4[\mathbf{1}]$ is capable of catalyzing sulfide oxidation with H_2O_2 in aqueous medium. For example, in $\text{MeCN}/\text{H}_2\text{O}$ (1 : 1, v/v), in the presence of 2 mol% of $\text{Na}_4[\mathbf{1}]$, methyl *p*-tolyl sulfide was oxidized by H_2O_2 to afford methyl *p*-tolyl sulfoxide selectively in 95% yield. Electrospray ionization mass spectrometry indicated that the reaction of $\text{Na}_4[\mathbf{1}]$ with H_2O_2 generated new species with $m/z = 430.2228$ and 434.2198 corresponding to $[\mathbf{1} + \text{O}]^{4-}$ and $[\mathbf{1} + 2\text{O}]^{4-}$, respectively, which are possible active intermediates in the catalytic sulfide oxidation.

Received 24th March 2025,

Accepted 7th May 2025

DOI: 10.1039/d5dt00712g

rsc.li/dalton

Introduction

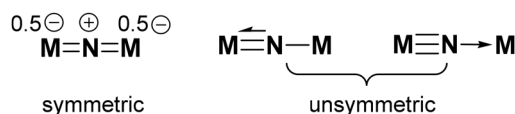
Nitride (N^{3-}) is a good supporting ligand for high-valent transition metal ions owing to its strong π -donating capability. As a bridging ligand, it can bind to two metal ions in either a symmetric or unsymmetric fashion depending upon the extent of π delocalization in the M–N–M' unit (Scheme 1).¹ Of interest are dinuclear iron complexes with symmetric nitrido bridges, such as $[\text{Fe}(\text{L})]_2(\mu\text{-N})$ (L^{2-} = phthalocyanine or a porphyrin dianion), which are capable of catalyzing C–H oxidation of hydrocarbons, including methane, with H_2O_2 or alkyl hydroperoxides,^{2–12} in which high-valent diiron-oxo species (“Fe=N–Fe=O”) have been proposed to be the active oxidants. It has been suggested that the enhanced oxidation capability of the diiron-oxo active species originates from the π -donation

of the μ -nitrido ligand that increases the basicity of the Fe=O group and facilitates the H-atom abstraction.^{13,14} Nevertheless, the catalytic activity of analogous heterometallic Fe–N–M complexes has not been explored.^{14,15}

In previous work, we have synthesized a series of heterometallic Fe–N–Ru complexes *via* the reactions of a Ru(VI) terminal nitride, $[\text{Ru}(\text{LOEt})(\text{N})\text{Cl}_2]$ ($\text{LOEt}^- = [(\eta^5\text{-C}_5\text{H}_5)\text{Co}\{\text{P}(\text{O})(\text{OEt})_2\}_3]^-$), with Fe(II) complexes bearing macrocyclic ligands, including porphyrin, phthalocyanine, and tetradentate Schiff base ligands (Scheme 2).^{16–18} X-ray diffraction studies revealed that these heterometallic complexes possess M=N double bonds that are indicative of the Fe(IV)=N= Ru(IV) resonance structure. Although they exhibit well-defined oxidation couples in the cyclic voltammograms (CVs), attempts to synthesize high-valent heterometallic nitrido complexes were unsuccessful. For

Department of Chemistry, The Hong Kong University of Science and Technology, Clear Water Bay, Kowloon, Hong Kong, China. E-mail: chanwan@ust.hk, chwill@ust.hk, chleung@ust.hk

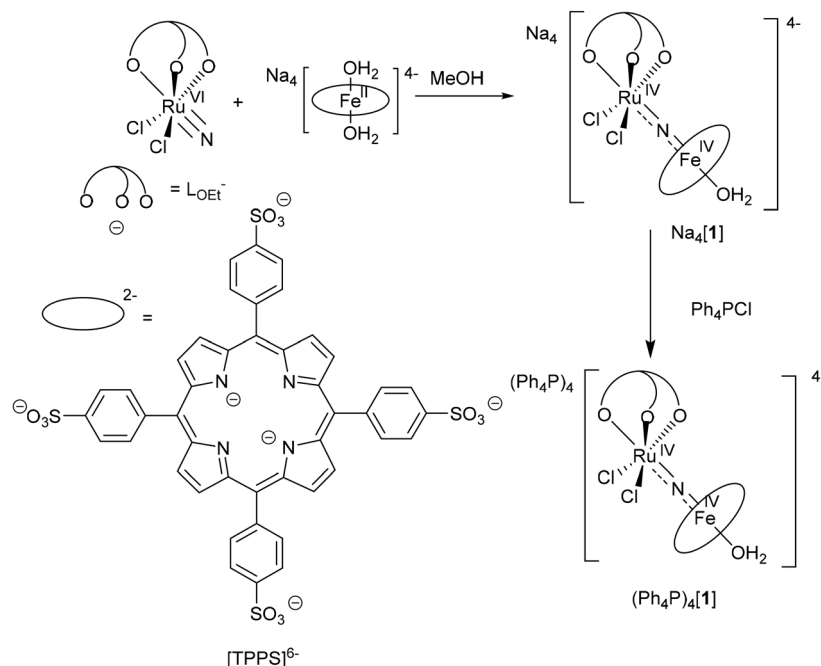
† Electronic supplementary information (ESI) available: Syntheses of $\text{Na}_4[\mathbf{1}\text{-Me}]$ and $\mathbf{2}\text{-TPP}$, NMR, UV-visible and mass spectra, cyclic voltammograms and X-ray crystallographic data. CCDC 2417666. For ESI and crystallographic data in CIF or other electronic format see DOI: <https://doi.org/10.1039/d5dt00712g>



Scheme 1 Dinuclear μ -nitrido complexes with symmetric and unsymmetric nitrido bridges.



Treatment of a suspension of $\text{Na}_4[\text{Fe}(\text{TPPS})(\text{H}_2\text{O})_2]$ ³⁹ in methanol with $[\text{Ru}(\text{L}_{\text{OEt}})(\text{N})\text{Cl}_2]$ resulted in the formation of a heterometallic nitrido complex, $\text{Na}_4[(\text{H}_2\text{O})(\text{TPPS})\text{Fe}(\mu\text{-N})\text{RuCl}_2(\text{L}_{\text{OEt}})]$ ($\text{Na}_4[\mathbf{1}]$) (Scheme 3). Unlike $\text{Na}_4[\text{Fe}(\text{TPPS})(\text{H}_2\text{O})_2]$, which is sparingly soluble in methanol, $\text{Na}_4[\mathbf{1}]$ is soluble in both water and methanol, but it is insoluble in acetonitrile or acetone. The ^1H NMR spectrum of $\text{Na}_4[\mathbf{1}]$ in D_2O showed sharp peaks that can be assigned to the TPPS^{4-} and L_{OEt}^- ligands in normal regions, which is indicative of its diamagnetic behavior. The UV/visible spectrum in water displayed the porphyrin Soret and Q bands at 425 and 548 nm, respectively, which are red-shifted compared with $\text{Na}_4[\text{Fe}(\text{TPPS})(\text{H}_2\text{O})_2]$ (413 and 517 nm, respectively). The ESI mass spectrum of $\text{Na}_4[\mathbf{1}]$ in



Scheme 3 Synthesis of Fe(IV)–Ru(IV) nitrido TPPS complexes.

water showed a signal at $m/z = 426.2221$ corresponding to $[1]^{4-}$ (Fig. S13, ESI†). Despite many attempts, we have not been able to obtain single crystals of Na₄[1] for structure determination. We have also synthesized the L_{OMe}[−] analogue of Na₄[1], Na₄[1-Me], from Na₄[Fe(TPPS)(H₂O)₂] and [Ru(N)(L_{OMe})Cl₂] (L_{OMe}[−] = $[(\eta^5\text{-C}_5\text{H}_5)\text{Co}\{\text{P}(\text{O})(\text{OMe})_2\}_3]^-$). Recrystallization of Na₄[1-Me] from MeOH/MeCN/acetone afforded red single crystals, which were identified as the heterometallic Fe–N–Ru complex $[\text{H}][\text{Na}_3(\text{Me}_2\text{CO})(\text{MeOH})(\text{H}_2\text{O})][(\text{MeOH})(\text{TPPS})\text{Fe}(\mu\text{-N})\text{RuCl}_2(\text{L}_{\text{OMe}})]$ according to an X-ray diffraction study (Fig. S1, ESI†). However, the bond lengths and angles of the L_{OMe}[−] complex have not been analyzed owing to serious disorder problems.

Cation metathesis of Na₄[1] with PPh₄Cl in methanol led to the isolation of $[(\text{Ph}_4\text{P})_4][(\text{H}_2\text{O})(\text{TPPS})\text{Fe}(\mu\text{-N})\text{RuCl}_2(\text{L}_{\text{OMe}})]$, (Ph₄P)₄[1], which is soluble in organic solvents such as CH₂Cl₂. Recrystallization from CH₂Cl₂/Et₂O/hexane afforded dark red crystals, which were suitable for X-ray diffraction. To our knowledge, (Ph₄P)₄[1] is the first structurally characterized Fe(TPPS) nitrido complex. It should be noted that very few crystal structures of Fe(TPPS) complexes have been reported in the literature.⁴⁰ The structure of the complex anion in (Ph₄P)₄[1] is shown in Fig. 1. Displacements of atoms from the porphyrin N4 plane are given in Fig. 2. The porphyrin macrocycle displays a saddled distortion. The Fe–N(porphyrin) distances [av. 2.003 Å] are similar to those of $[(\text{py})(\text{TPP})\text{Fe}(\mu\text{-N})\text{Ru}(\text{L}_{\text{OMe}})\text{Cl}_2]$ (py = pyridine) (1.997 Å)¹⁶ but shorter than those of $[\{\text{Fe}(\text{TPPS})\}_2(\mu\text{-O})]^{8-}$ (av. 2.079 Å).⁴⁰ The Fe–OH₂ distance of 2.069(4) Å is similar to that of the Pc complex $[(\text{H}_2\text{O})(\text{Pc})\text{Fe}(\mu\text{-N})\text{RuCl}_2(\text{L}_{\text{OMe}})]$ [2.046(5) Å].¹⁷ The Fe–N(nitrido) [1.676(5) Å] and Ru–N(nitrido) [1.701(5) Å] distances in $[1]^{4-}$ compare well

with those of $[(\text{py})(\text{TPP})\text{Fe}(\mu\text{-N})\text{Ru}(\text{L}_{\text{OMe}})\text{Cl}_2]$ [1.683(3) and 1.704(3) Å, respectively].¹⁶ The Fe–N–Ru unit is roughly linear with a bond angle of 171.4(3)°. The observed short M–N(nitride) bond distances and diamagnetism of $[1]^{4-}$ are indicative of the Fe(IV)=N=Ru(IV) bonding behavior.

Electrochemistry

The CV of Na₄[1] in 0.1 M HCl (pH 1) displayed two reversible oxidation couples at +0.66 and +0.94 V *versus* the saturated calomel electrode (SCE) (Fig. 3). To gain insight into the nature of the first couple, the oxidation of Na₄[1] with a 1-electron oxidant, cerium(IV) ammonium nitrate $[(\text{NH}_4)_2[\text{Ce}(\text{NO}_3)_6]]$ (CAN), which has a redox potential of +0.88 V *versus* SCE,⁴¹ was studied. Treatment of Na₄[1] with 1 equivalent of CAN in water resulted in a blue-shift of the Soret band from 425 to 398 nm in the UV/visible spectrum (Fig. 4). A similar spectral change was found for the oxidation of Na₄[1] with CAN in 0.1 M HCl. No absorption at ~800 nm that is characteristic of a porphyrin radical cation was found, suggesting that the oxidation at +0.66 V is a metal-centred event, either Fe(v/IV), Ru(v/IV) or a combination of both. No further spectral change was found when excess (>3 equivalents) CAN was added. The nature of the second redox couple is unclear, but it is very likely that it resulted from a porphyrin-based oxidation. When the pH was increased to 3, similar half-wave potentials were found for the two redox couples, but they were less reversible (Fig. 5). At pH 6, only irreversible oxidation waves were found (Fig. 6). In contrast, the CV of (Ph₄P)₄[1] in CH₂Cl₂ displayed an irreversible oxidation wave with $E_{\text{pa}} = +0.51$ V *versus* Fc⁺⁰ (Fc = ferrocene) (Fig. S11, ESI†), whereas the reported compound $[(\text{py})(\text{TPP})\text{Fe}$

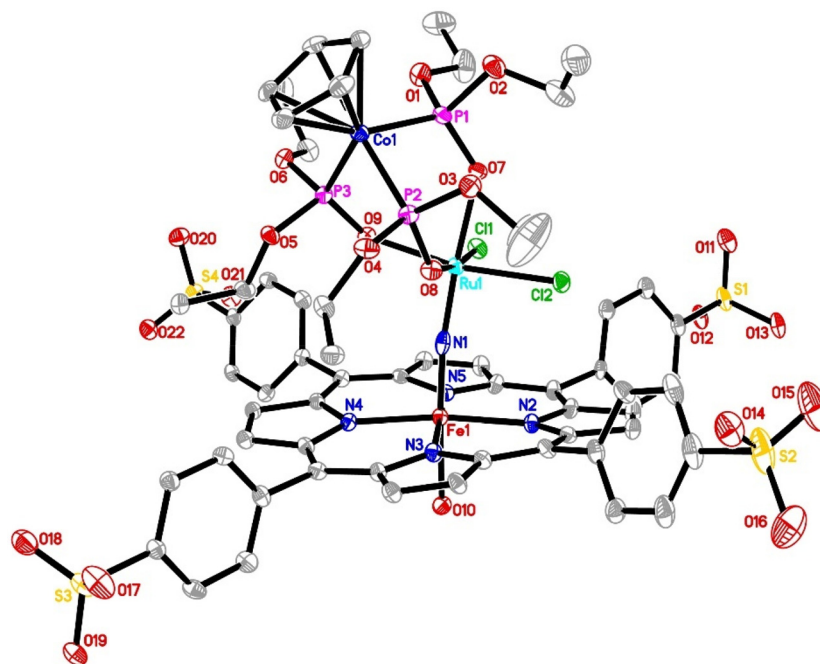


Fig. 1 Molecular structure of the tetra-anion $[1]^{4-}$. Hydrogen atoms are omitted for clarity. The ellipsoids are drawn at the 30% possibility level. Selected bond lengths (Å) and angles (°): Fe1–N1: 1.676(5); Fe1–N2: 2.006(4); Fe1–N3: 1.997(4); Fe1–N4: 2.016(4); Fe1–N5: 1.994(4); Fe1–O10: 2.069(4); Ru1–N1: 1.701(5); Ru1–Cl1: 2.3284(13); Ru1–Cl2: 2.3412(13); Ru1–O7: 2.124(3); Ru1–O8: 2.075(4); Ru1–O9: 2.068(3); Fe1–N1–Ru1 171.4(3).

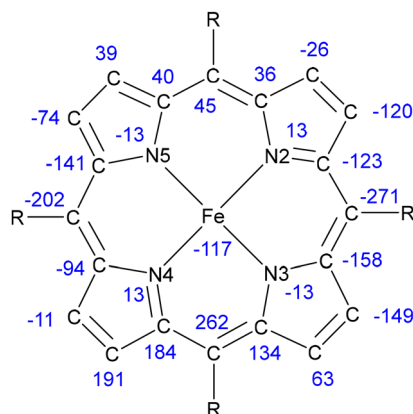


Fig. 2 Atomic displacements (10^{-3} Å) from the porphyrin N4 plane in $[1]^{4-}$.

$(\mu\text{-N})\text{Ru}(\text{LOEt})\text{Cl}_2$ exhibited two oxidation events at +0.29 and +0.77 V in CH_2Cl_2 .¹⁶

Reaction of $\text{Na}_4[1]$ with oxidizing agents

Attempts have been made to synthesize high-valent heterometallic nitrido complexes by chemical oxidation of $\text{Na}_4[1]$. Treatment of $\text{Na}_4[1]$ with 1 equivalent of AgNO_3 in water resulted in a red-shift of the Soret band from 425 to *ca.* 440 nm (see the ESI†). No AgCl precipitate was found, indicating that the $\text{Ag}(\text{i})$ ion did not abstract the chloride ion at the Ru center. Attempts to isolate the product by adding excess acetone to the aqueous reaction mixture failed. To increase the

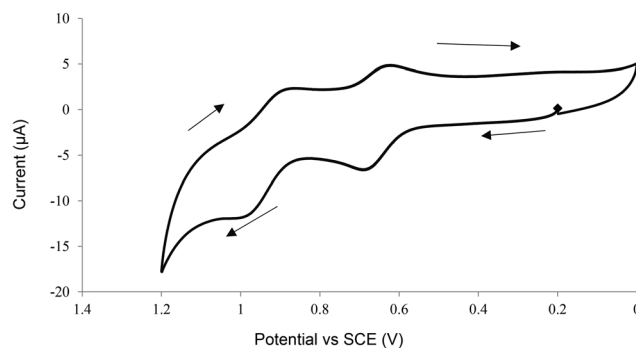


Fig. 3 CV of $\text{Na}_4[1]$ in 0.1 M HCl (pH 1). Working electrode: glassy carbon, reference electrode: standard calomel electrode, scan rate = 100 mV s^{-1} .

solubility of the product in organic solvents, $[1]^{4-}$ was reacted with $\text{Ag}(\text{i})$ in the presence of a ligand that can bind to the Fe center. Thus, treatment of $\text{Na}_4[1]$ with $\text{Ag}(\text{CF}_3\text{SO}_3)$ in methanol, followed by the addition of PPh_3 , led to the isolation of red crystals that were characterized as $\text{Na}_3[(\text{H}_2\text{O})(\text{TPPS})\text{Fe}(\mu\text{-N})\text{Ru}(\text{LOEt})\text{Cl}_2\{\text{Ag}(\text{PPh}_3)\}](\text{CF}_3\text{SO}_3)$ (**2**) (Scheme 4). The ^1H NMR spectrum of **2** showed resonances that can be attributed to the TPPS^{4-} , LOEt^- and PPh_3 ligands, indicative of the diamagnetic properties. The $^{31}\text{P}\{^1\text{H}\}$ NMR spectrum showed a resonance at δ 15.99 ppm due to the Ag-bound PPh_3 ligand. We have not been able to crystallize **2** for structure determination. However, we have structurally characterized the TPP analogue of **2**, $[(\text{TPP})\text{Fe}(\mu\text{-N})\text{Ru}(\text{LOEt})\text{Cl}_2\{\text{Ag}(\text{PPh}_3)\}](\text{CF}_3\text{SO}_3)$ (**2-TPP**), which was synthesized from $[(\text{TPP})\text{Fe}(\mu\text{-N})\text{Ru}(\text{LOEt})\text{Cl}_2]$, $\text{Ag}(\text{CF}_3\text{SO}_3)$



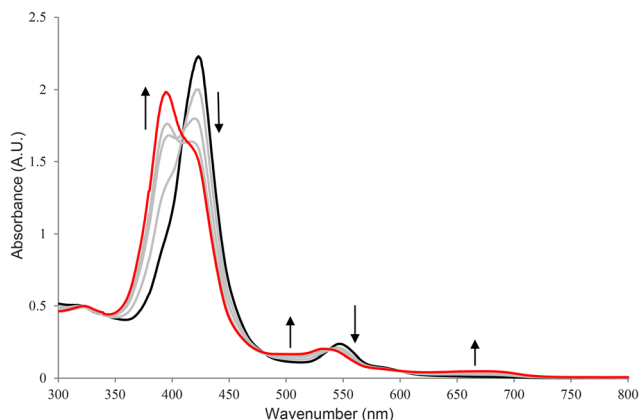


Fig. 4 UV/visible spectral change for the reaction of $\text{Na}_4[1]$ with 1 equivalent of CAN in water at room temperature. 1/4 equiv. of CAN was added in each scan.

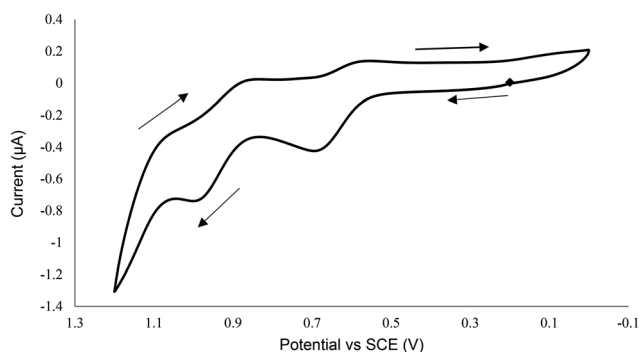


Fig. 5 CV of $\text{Na}_4[1]$ at pH 3. Working electrode: glassy carbon, reference electrode: standard calomel electrode, scan rate = 100 mV s^{-1} .

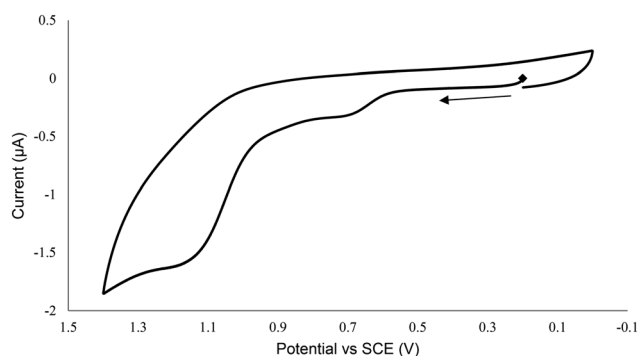
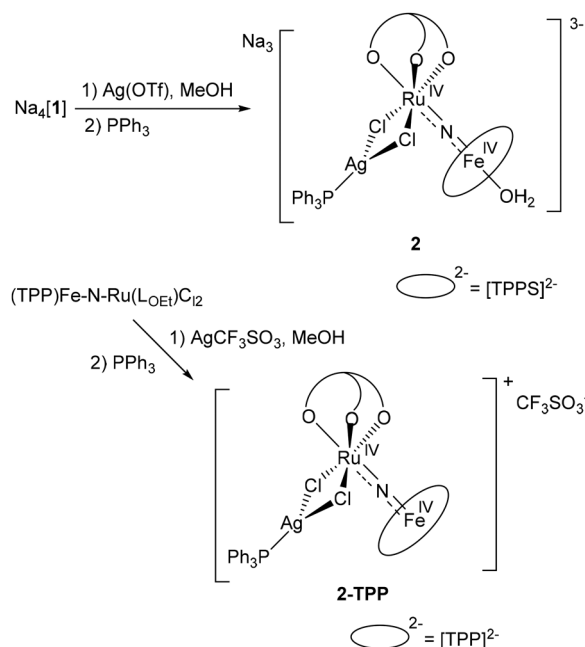


Fig. 6 CV of $\text{Na}_4[1]$ at pH 6. Working electrode: glassy carbon, reference electrode: standard calomel electrode, scan rate = 100 mV s^{-1} .

and PPh_3 (Scheme 4). A preliminary X-ray diffraction study revealed that the $[\text{Ag}(\text{PPh}_3)]^+$ unit binds to the two chloride ligands of the $[\text{Ru}(\text{LOEt})\text{Cl}_2]$ moiety in **2-TPP** (Fig. S3, ESI†). We believe that **2** has a core structure similar to **2-TPP** featuring $\text{Ru}(\mu\text{-Cl})\text{Ag}$ bridges. Thus, instead of oxidizing the metal centers, the $\text{Ag}(\text{I})$ ion binds to the chloride ligands in $[1]^{4-}$.



Scheme 4 Reactions of Fe-N-Ru porphyrin complexes with $\text{Ag}(\text{I})$ and PPh_3 .

As mentioned earlier, the oxidation of $\text{Na}_4[1]$ with CAN in water gave a high-valent species that displayed absorption bands at 398 and 507 nm in the UV/visible spectrum. Attempts to precipitate this species by the addition of acetone to the aqueous reaction mixture failed.

When $\text{Na}_4[1]$ in water at room temperature was treated with 1 equivalent of H_2O_2 , no significant change was found in the UV/visible spectrum, but some gas bubbles, presumably oxygen, were observed. When excess H_2O_2 (>10 equivalents) was added, new absorption bands centred at 398 and 515 nm that are similar to those found for the CAN oxidation of $[1]^{4-}$ appeared, suggesting that a high-valent species, possibly an $\text{Fe}(\text{v})$ or $\text{Ru}(\text{v})$ complex, was generated. When $\text{Na}_4[1]$ was reacted with H_2O_2 in methanol, the same spectral change was found. Upon addition of excess methyl *p*-tolyl sulfide (20 equivalents) to the methanol

Table 1 Catalytic sulfide oxidation with H_2O_2 ^a

$p\text{-tol-S} \xrightarrow[\text{solvent, rt, air, 3h}]{\text{H}_2\text{O}_2, 2 \text{ mol\% cat.}} p\text{-tol-S(=O)}$			
Entry	Catalyst	Solvent	% yield ^b
1	$\text{Na}_4[1]$	$\text{MeCN}/\text{H}_2\text{O}$ (v/v, 1 : 1)	95 ^c
2	$\text{Na}_4[1]$	MeOH	92 ^c
3	$(\text{Ph}_4\text{P})_4[1]$	CH_2Cl_2	5
4	2	$\text{MeCN}/\text{H}_2\text{O}$ (v/v, 1 : 1)	25

^a Experimental conditions: catalyst (1 μmol), methyl *p*-tolyl sulfide (0.1 mmol) and H_2O_2 (50 μmol) were stirred at room temperature in air for 3 h. ^b Yield determined by GC-FID using bromobenzene as the internal standard. ^c A trace amount of sulfone was detected.

solution, methyl *p*-tolyl sulfoxide that was identified by GC-MS was formed, but there was no change in the Soret band at 398 nm, indicating that this high-valent species was not involved in the sulfide oxidation. However, when a large excess of methyl *p*-tolyl sulfide (200 equivalents) was added to the mixture, the absorption peak at 398 nm dropped slowly and the Soret band of $[1]^{4-}$ (425 nm) appeared (Fig. S9, ESI†). Therefore, in the presence of a large excess of thioether, this high-valent species will also be slowly reduced to $[1]^{4-}$.

Catalytic sulfide oxidation with H_2O_2

The above results indicate that the reaction of $[1]^{4-}$ with H_2O_2 generated a reactive species that is capable of OAT. The use of $[1]^{4-}$ as a catalyst for sulfide oxidation with H_2O_2 has been explored, and the results are summarized in Table 1. Treatment of methyl *p*-tolyl sulfide with H_2O_2 in MeCN/ H_2O (1 : 1, v/v) in the presence of 2 mol% of $Na_4[1]$ afforded methyl *p*-tolylsulfoxide selectively in 95% yield. Only a trace amount of

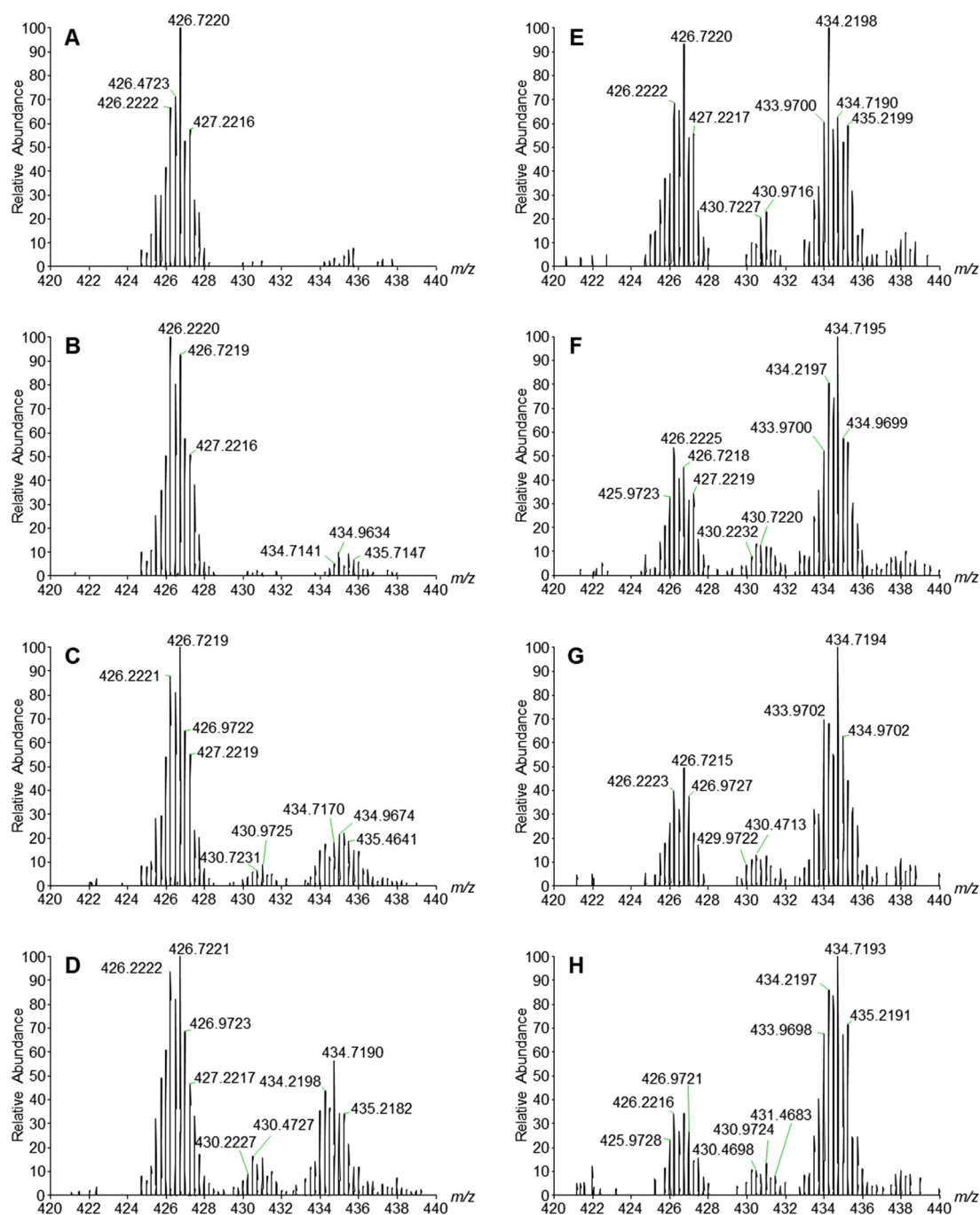


Fig. 7 ESI-MS monitoring of the formation of $[1 + O]^{4-}$ (m/z 430.2228) and $[1 + 2O]^{4-}$ (m/z 434.2198) species via the reaction of $[1]^{4-}$ with H_2O_2 (10 equivalents) in water at room temperature at $t = 0$ (A), 8 (B), 16 (C), 22 (D), 30 (E), 41 (F), 47 (G), and 55 (H) min.



sulfone was detected. A similar yield (92%) was obtained when methanol was used as the solvent. However, only 5% of sulfoxide was formed when the oxidation was carried out in CH_2Cl_2 using $(\text{Ph}_4\text{P})_4[\mathbf{1}]$ as a catalyst, indicating that the aqueous medium favors the catalytic oxidation of the heterometallic nitrido complex. The reduced catalytic activity of the $[\text{PPh}_4]^+$ salt can be attributed to the high oxidation potential of $[\mathbf{1}]^{4-}$ in CH_2Cl_2 (+0.51 V *versus* $\text{Fc}^{+/0}$), which renders the generation of a high-valent active species difficult. Similarly, the binding of the cationic $[\text{Ag}(\text{PPh}_3)]^+$ moiety has a negative impact on the performance of the Fe/Ru catalyst; the yield of sulfoxide was decreased to 25% when trianionic $\mathbf{2}$ was used as the catalyst.

MS monitoring of the reaction of $\text{Na}_4[\mathbf{1}]$ with H_2O_2

The reaction of $\text{Na}_4[\mathbf{1}]$ with H_2O_2 has been monitored by ESI-MS in the range of m/z 420–440 (Fig. 7). Upon addition of *ca.* 10 equivalents of H_2O_2 , a new signal at m/z 434.2198, which can be assigned to $[\mathbf{1} + 2\text{O}]^{4-}$ (Fig. S14, ESI[†]), was observed. The intensity of the $[\mathbf{1}]^{4-}$ signal decreased gradually as the $[\mathbf{1} + 2\text{O}]^{4-}$ peak rose. At about 16 min, a new signal at m/z 430.2228 that is attributed to $[\mathbf{1} + \text{O}]^{4-}$ (Fig. S15, ESI[†]) appeared. After 56 min, the $[\mathbf{1} + 2\text{O}]^{4-}$ peak became the predominant signal in the mass spectrum. It seems reasonable to assume that the reaction of $[\mathbf{1}]^{4-}$ with H_2O_2 afforded $[\mathbf{1} + 2\text{O}]^{4-}$, which was subsequently converted to $[\mathbf{1} + \text{O}]^{4-}$.

A previous work has shown that the active oxidants of diiron-catalyzed oxidations with H_2O_2 are high-valent diiron-oxo species, which are formed *via* heterolytic O–O cleavage of (hydro)peroxo intermediates.⁸ We therefore assign the MS signals at m/z 434.2198 and 430.2228 as heterometallic Ru/Fe peroxo and oxo species, respectively. A possible mechanism for the catalytic sulfoxidation with $[\mathbf{1}]^{4-}$ is shown in Scheme 5. Reaction of $[\mathbf{1}]^{4-}$ with H_2O_2 generates a peroxo intermediate, **I**, which in the absence of a substrate decomposes to $[\mathbf{1}]^{4-}$ readily. If excess H_2O_2 is used, a sufficient amount of **I** is accumulated, and it can be observed in ESI-MS. Subsequently, O–O

cleavage of **I** affords a reactive dimetallic oxo species, **II**, which is the active oxidant for the sulfoxidation. The reaction of $[\mathbf{1}]^{4-}$ with excess H_2O_2 also generates a high-valent species, possibly an Fe(v) or Ru(v) complex, *via* another pathway that is not clear at this stage. This high-valent species is, however, unable to undergo OAT with the thioether.

Conclusions

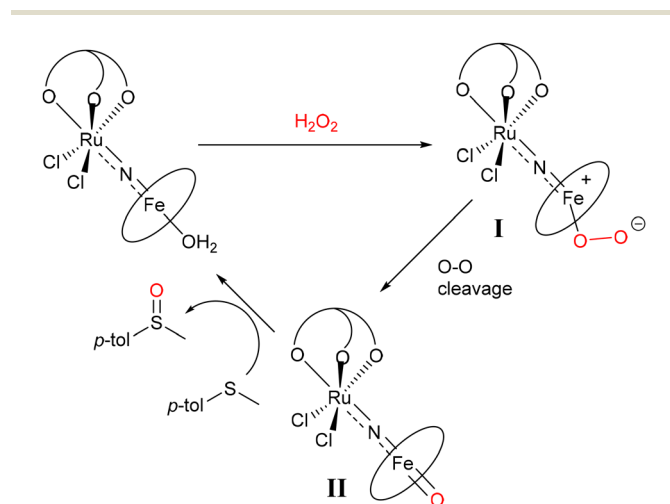
We have synthesized a heterometallic Ru(IV)–Fe(IV) nitrido complex bearing a water-soluble porphyrin, $[\mathbf{1}]^{4-}$. $(\text{Ph}_4\text{P})_4[\mathbf{1}]$ is the first Fe(IV) TPPS nitrido complex that has been characterized by X-ray diffraction. The binding of the Ru(VI) nitride moiety to $[\text{Fe}(\text{TPPS})]^{4-}$ not only increases the solubility of the TPPS complex in organic solvents, facilitating its isolation and crystallization, but also inhibits its aggregation in aqueous solution. This strategy can be exploited for isolation and crystallization of other water-soluble metalloporphyrins in aqueous media. $[\mathbf{1}]^{4-}$ undergoes 1-electron oxidation at a relatively low potential ($E_2 = +0.66$ V *versus* SCE) in an acidic solution to yield a high-valent heterometallic nitrido complex that has an overall d^7 configuration. $[\mathbf{1}]^{4-}$ proved to be an efficient catalyst for sulfide oxidation with H_2O_2 in aqueous media. ESI-MS indicated that the oxidation of $[\mathbf{1}]^{4-}$ with H_2O_2 produced peroxo and oxo species. It is believed that O–O cleavage of the peroxo intermediate generates an heterometallic oxo species, which is the active species for the sulfide oxidation. The results of this work demonstrate the potential application of water-soluble heterometallic nitrido complexes in catalytic OAT reactions in aqueous media.

Experimental

General information

All manipulations were performed under nitrogen using standard Schlenk techniques. NMR spectra were recorded on a Bruker ARX 400 spectrometer operating at 400, 376.5, and 162 MHz for ^1H , ^{19}F , and ^{31}P , respectively. Chemical shifts (δ , ppm) were reported with reference to SiMe_4 (^1H), $\text{CF}_3\text{C}_6\text{H}_5$ (^{19}F), and H_3PO_4 (^{31}P). UV-visible spectra were recorded on a Dynamica HALO DB-20 spectrometer. ESI mass spectrometry was performed on an UltiMate 3000 UHPLC system coupled with an Orbitrap Exploris™ 120 mass spectrometer (Thermo Fisher, Waltham, MA). Cyclic voltammetry was performed with a CH Instrument model 600D potentiostat. The reference electrodes for aqueous and non-aqueous studies were the standard calomel electrode and $\text{Ag}–\text{AgNO}_3$ (0.1 M in acetonitrile) electrodes, respectively. Elemental analyses were performed by Medac Ltd, Surrey, UK. The compounds $\text{Na}_4[\text{Fe}(\text{TPPS})(\text{H}_2\text{O})_2]$ ³⁹ and $[\text{Ru}(\text{LOEt})(\text{N})\text{Cl}_2]$ ⁴² were prepared according to literature methods. Other reagents were purchased from Aldrich Ltd and used as received.

Preparation of $\text{Na}_4[(\text{H}_2\text{O})\text{Fe}(\text{TPPS})(\mu\text{-N})\text{RuCl}_2\text{LOEt}]$ ($\text{Na}_4[\mathbf{1}]$). To a suspension of $\text{Na}_4[\text{Fe}(\text{TPPS})(\text{H}_2\text{O})_2]$ (50 mg, 0.045 mmol)



Scheme 5 Proposed mechanism for the $[\mathbf{1}]^{4-}$ -catalyzed sulfide oxidation.



in MeOH (10 mL) was added 1 equivalent of $[\text{Ru}(\text{N})(\text{L}_{\text{OEt}})\text{Cl}_2]$ (32 mg, 0.045 mmol), and the reaction mixture was stirred at room temperature overnight. The solvent was pumped off, and the residue was extracted with MeOH/MeCN (5 mL, 1 : 3 v/v). Recrystallization from MeOH/MeCN/acetone afforded red crystals. Yield: 39 mg, 50%. ^1H NMR (400 MHz, D_2O): δ 0.81 (t, J = 7.2 Hz, 6H, CH_3), 0.89 (t, J = 7.2 Hz, 6H, CH_3), 1.14 (t, J = 7.2 Hz, 6H, CH_3), 2.44 (m, 4H, CH_2), 3.34 (m, 4H, CH_2), 4.66 (s, 5H, Cp), 8.22 (d, J = 8.4 Hz, 8H, H_m), 8.41 (m, 8H, H_o), 9.03 (s, 8H, $\text{H}_{\text{pyrrole}}$). $^{31}\text{P}\{^1\text{H}\}$ NMR (162 MHz, D_2O): δ 117.79 (m). MS-ESI: m/z 426 $[\text{1} - \text{H}_2\text{O}]^{4-}$. Anal. calc. for $\text{C}_{61}\text{H}_{61}\text{Cl}_2\text{CoFeN}_5\text{Na}_4\text{O}_{22}\text{P}_3\text{RuS}_4 \cdot 9\text{H}_2\text{O}$: C, 37.04; H, 4.03; N, 3.54. Found: C, 37.11; H, 3.86; N, 4.08.

Preparation of $(\text{Ph}_4\text{P})_4[(\text{H}_2\text{O})(\text{TPPS})\text{Fe}(\mu\text{-N})\text{RuCl}_2\text{L}_{\text{OEt}}](\text{PPh}_4)_4[\text{1}]$. To a suspension of $\text{Na}_4[\text{1}]$ (50 mg, 0.029 mmol) in MeOH (5 mL) were added 4 equivalents of $\text{Ph}_4\text{P}\text{Cl}$ (44 mg, 0.12 mmol). The solvent was pumped off, and the residue was washed with water and dried *in vacuo*. Recrystallization from $\text{CH}_2\text{Cl}_2/\text{Et}_2\text{O}/\text{hexane}$ gave dark red single crystals. Yield: 43 mg, 48%. ^1H NMR (400 MHz, CDCl_3): δ 0.68 (t, J = 7.2 Hz, 6H, CH_3), 0.91 (t, J = 7.2 Hz, 6H, CH_3), 1.08 (t, J = 7.2 Hz, 6H, CH_3), 2.27 (m, 3H, CH_2), 2.41 (m, 3H, CH_2), 3.28 (q, J = 7.2 Hz, 6H, CH_2), 4.49 (s, 5H, Cp), 7.84 (m, 65H, Ph), 7.97 (m, 19H, Ph), 8.10 (m, 12H, Ph), 8.76 (s, 8H, $\text{H}_{\text{pyrrole}}$). $^{31}\text{P}\{^1\text{H}\}$ NMR (162 MHz, CDCl_3): δ 22.91 (s, PPh_4^+), 117.14 (m, L_{OEt}^-). Anal. calc. for $\text{C}_{157}\text{H}_{160}\text{Cl}_2\text{CoFeN}_5\text{O}_{32}\text{P}_7\text{RuS}_4$: C, 57.83; H, 4.95; N, 2.15. Found: C, 57.85; H, 4.87; N, 2.33.

Preparation of $\text{Na}_3[(\text{H}_2\text{O})(\text{TPPS})\text{Fe}(\mu\text{-N})\text{Ru}(\text{L}_{\text{OEt}})\text{Cl}_2\{\text{Ag}(\text{PPh}_3)\}]$ (2). To a solution of $\text{Na}_4[\text{1}]$ (50 mg, 0.029 mmol) in MeOH (5 mL) were added AgCF_3SO_3 (7.5 mg, 0.029 mmol) and PPh_3 (6.4 mg, 0.029 mmol), and the mixture was stirred overnight at room temperature and filtered. The solvent was pumped off, and the residue was extracted with MeOH/MeCN (5 mL, 1 : 3 v/v). Recrystallization from MeOH/MeCN/acetone afforded red crystals. Yield: 39 mg, 50%. ^1H NMR (400 MHz, D_2O): δ 0.58 (overlapping t, 6H, CH_3), 0.83 (overlapping t, 6H, CH_3), 1.01 (overlapping t, 6H, CH_3), 2.43 (m, 2H, CH_2), 2.55 (m, 2H, CH_2), 3.25 (m, 8H, CH_2), 4.66 (s, 5H, Cp), 7.26 (m, 5H, Ph), 7.40 (m, 5H, Ph), 7.51 (m, 3H, Ph), 8.18 (m, 10H, Ph and H_m), 8.37 (m, 8H, H_o), 9.01 (s, 8H, $\text{H}_{\text{pyrrole}}$). $^{31}\text{P}\{^1\text{H}\}$ NMR (162 MHz, D_2O): δ 15.99 (dd, $^1J(^{31}\text{P}-^{107}\text{Ag}) = 654$ Hz, $^1J(^{31}\text{P}-^{109}\text{Ag}) = 755$ Hz, PPh_3), 117.79 (m, L_{OEt}^-). Anal. calc. for $\text{C}_{79}\text{H}_{74}\text{AgCl}_2\text{CoFeN}_5\text{Na}_3\text{O}_{21}\text{P}_4\text{RuS}_4 \cdot 8\text{H}_2\text{O}$: C, 41.45; H, 3.96; N, 3.06. Found: C, 38.39; H, 3.79; N, 2.88.

Catalytic oxidation of *p*-tolyl methyl sulfide with H_2O_2 . To a solution of *p*-tolyl methyl sulfide (0.1 mmol) and $\text{Na}_4[\text{1}]$ (1 μmol) in water (10 mL) was added H_2O_2 (50 mmol), and the mixture was stirred at room temperature in air for 3 h. The yield of *p*-tolyl methyl sulfoxide was determined by GLC using bromobenzene as the internal standard.

ESI-MS monitoring of the reaction of $\text{Na}_4[\text{1}]$ with H_2O_2 in water. To a solution of $\text{Na}_4[\text{1}]$ in double deionized water (950 μL , 6.5 μM) was added aqueous H_2O_2 (50 μL , 1.1 mM). The resulting mixture was subjected to MS analysis at t = 0, 8, 16, 22, 30, 41, 47, and 55 min.

X-ray crystallography

Crystallographic data and experimental details for $[\text{Ph}_4\text{P}]_4[\text{1}]$ are summarized in Table S1 (ESI[†]). Intensity data of the complexes were collected with a Rigaku SuperNova Atlas X-ray diffractometer using graphite-monochromated Cu-K α radiation. The collected frames were processed using CrysAlisPro software. Using Olex2,⁴³ the structure was solved with the SHELXT⁴⁴ structure solution program using intrinsic phasing and refined with the SHELXL⁴⁵ refinement package using least squares minimisation. Atomic positions of non-hydrogen atoms were refined anisotropically and with restraints applied to those disordered atoms. Hydrogen atoms were refined as riding on their respective parent atoms before the final cycle of least-squares refinement. Disorder is found in some solvent molecules in the structure. However, as the disorder does not affect the interpretation of the overall structure of the compound, no further modeling was made.

Data availability

The data supporting this article, including syntheses of $\text{Na}_4[\text{1-Me}]$ and 2-TPP, NMR, UV-visible and mass spectra, cyclic voltammograms and X-ray crystallographic data, have been included as part of the ESI[†]. Crystallographic data for $(\text{PPh}_4)_4[\text{1}]$ have been deposited at the CCDC under CCDC 2417666.[†]

Conflicts of interest

There are no conflicts to declare.

Acknowledgements

This work was supported by the Hong Kong Research Grants Council (project numbers 16301120, 16301621 and 16301424) and the Hong Kong University of Science and Technology.

References

- 1 K. Dehnicke and J. Strähle, *Angew. Chem., Int. Ed. Engl.*, 1992, **31**, 955–978.
- 2 P. Afanasiev and A. B. Sorokin, *Acc. Chem. Res.*, 2016, **49**, 583–593.
- 3 A. B. Sorokin, *Adv. Inorg. Chem.*, 2017, **70**, 107–165.
- 4 A. B. Sorokin, *Catal. Today*, 2021, **373**, 38–58.
- 5 A. B. Sorokin, E. V. Kudrik and D. Bouchu, *Chem. Commun.*, 2008, 2562–2564.
- 6 E. V. Kudrik and A. B. Sorokin, *Chem. – Eur. J.*, 2008, **14**, 7123–7126.
- 7 E. V. Kudrik, P. Afanasiev, D. Bouchu, J. M. M. Millet and A. B. Sorokin, *J. Porphyrins Phthalocyanines*, 2008, **12**, 1078–1089.



- 8 E. V. Kudrik, P. Afanasiev, L. X. Alvarez, P. Dubourdeaux, M. Clémancey, M. J.-M. Latour, G. Blondin, D. Bouchu, F. Albrieux, S. E. Nefedov and A. B. Sorokin, *Nat. Chem.*, 2012, **4**, 1024–1029.
- 9 Y. Yamada, J. Kura, Y. Toyoda and K. Tanaka, *New J. Chem.*, 2020, **44**, 19179–19183.
- 10 Y. Yamada, K. Morita, N. Mihara, K. Igawa, K. Tomooka and K. Tanaka, *New J. Chem.*, 2019, **43**, 11477–11482.
- 11 Y. Yamada, Y. Miwa, Y. Toyoda, T. Yamaguchi, S. Akine and K. Tanaka, *Dalton Trans.*, 2021, **50**, 16775–16781.
- 12 Y. Yamada, Y. Miwa, Y. Toyoda, Y. Uno, Q. M. Phung and K. Tanaka, *Dalton Trans.*, 2024, **53**, 6556–6567.
- 13 M. G. Quesne, D. Senthilnathan, D. Singh, D. Kumar, P. Maldivi, A. B. Sorokin and S. P. de Visser, *ACS Catal.*, 2016, **6**, 2230–2243.
- 14 M. Q. E. Mubarak, A. B. Sorokin and S. P. de Visser, *JBIC, J. Biol. Inorg. Chem.*, 2019, **24**, 1127–1134.
- 15 S. A. Zdanovich, E. Y. Tyulyaeva, V. S. Sukharev, M. V. Zaitsev and S. V. Zaitseva, *Polyhedron*, 2025, **270**, 117448.
- 16 W.-M. Cheung, W.-H. Chiu, M. de Vere-Tucker, H. H.-Y. Sung, I. D. Williams and W.-H. Leung, *Inorg. Chem.*, 2017, **56**, 5680–5687.
- 17 W.-M. Cheung, W.-M. Ng, W.-H. Wong, H. K. Lee, H. H.-Y. Sung, I. D. Williams and W.-H. Leung, *Inorg. Chem.*, 2018, **57**, 9215–9222.
- 18 R. Ng, W.-M. Ng, W.-M. Cheung, H. H.-Y. Sung, I. D. Williams and W.-H. Leung, *J. Organomet. Chem.*, 2022, **967**, 122354.
- 19 D. R. Weinberg, C. J. Gagliardi, J. F. Hull, C. F. Murphy, C. A. Kent, B. C. Westlake, A. Paul, D. H. Ess, D. G. McCafferty and T. J. Meyer, *Chem. Rev.*, 2012, **112**, 4016–4093.
- 20 J. J. Warren, T. A. Tronic and J. M. Mayer, *Chem. Rev.*, 2010, **110**, 6961–7001.
- 21 C. Colombana, E. V. Kudrika, P. Afanasieva and A. B. Sorokin, *Catal. Today*, 2014, **235**, 14–19.
- 22 P. Hambright, in *The Porphyrin Handbook*, ed. K. Kaddish, K. M. Smith and R. Guilard, Academic Press, San Diego, 2000, vol. 3, ch. 18, pp. 129–210.
- 23 P. K. Pandey and G. Zheng, in *The Porphyrin Handbook*, ed. K. Kaddish, K. M. Smith and R. Guilard, Academic Press, San Diego, 2000, vol. 6, ch. 43, pp. 157–230.
- 24 P. Böhm and H. Gröger, *ChemCatChem*, 2015, **7**, 22–28.
- 25 J. W. Buchler, *J. Porphyrins Phthalocyanines*, 2004, **8**, 43–66.
- 26 G. Lente and J. H. Espenson, *Green Chem.*, 2005, **7**, 28–34.
- 27 M. Fukushima and K. Tatsumi, *Environ. Sci. Technol.*, 2005, **39**, 9337–9342.
- 28 K. Kano, Y. Itoh, H. Kitagishi, T. Hayashi and S. Hirota, *J. Am. Chem. Soc.*, 2008, **130**, 8006–8015.
- 29 H. Kitagishi, M. Tamaki, T. Ueda, S. Hirota, T. Ohta, Y. Naruta and K. Kano, *J. Am. Chem. Soc.*, 2010, **132**, 16730–16732.
- 30 T. Ueda, H. Kitagishi and K. Kano, *Inorg. Chem.*, 2014, **53**, 543–551.
- 31 H. Kitagishi, D. Shimoji, T. Ohta, R. Kamiya, Y. Kudo, A. Onoda, T. Hayashi, J. Weiss, J. A. Wytke and K. Kano, *Chem. Sci.*, 2018, **9**, 1989–1995.
- 32 C. Khin, J. Heinecke and P. C. Ford, *J. Am. Chem. Soc.*, 2008, **130**, 13830–13831.
- 33 J. Heinecke and P. C. Ford, *J. Am. Chem. Soc.*, 2010, **132**, 9240–9243.
- 34 M. P. Jensen and D. P. Riley, *Inorg. Chem.*, 2002, **41**, 4788–4797.
- 35 H. Maid, P. Böhm, S. M. Huber, W. Bauer, W. Hummel, N. Jux and H. Gröger, *Angew. Chem., Int. Ed.*, 2011, **50**, 2397–2400.
- 36 E. B. Fleischer, J. M. Palmer, T. S. Srivastava and A. Chatterjee, *J. Am. Chem. Soc.*, 1971, **93**, 3162–3167.
- 37 D. A. Summerville and I. A. Cohen, *J. Am. Chem. Soc.*, 1976, **98**, 1747.
- 38 M. Li, M. Shang, N. Ehlinger, C. E. Schulz and W. R. Scheidt, *Inorg. Chem.*, 2000, **39**, 580–583.
- 39 Z. Dong and P. J. Scammells, *J. Org. Chem.*, 2007, **72**, 9881–9885.
- 40 A. Mazzeo, C. Gaviglio, J. Pellegrino and F. Doctorovich, *Heliyon*, 2022, **8**, e09555.
- 41 N. G. Connelly and W. E. Geiger, *Chem. Rev.*, 1996, **96**, 877–910.
- 42 X.-Y. Yi, T. C. H. Lam, Y.-K. Sau, Q.-F. Zhang, I. D. Williams and W.-H. Leung, *Inorg. Chem.*, 2007, **46**, 7193–7198.
- 43 O. V. Dolomanov, L. J. Bourhis, R. J. Gildea, J. A. K. Howard and H. Puschmann, *Appl. Crystallogr.*, 2009, **42**, 339–341.
- 44 G. M. Sheldrick, *Acta Crystallogr., Sect. A: Found. Adv.*, 2005, **71**, 3–8.
- 45 G. M. Sheldrick, *Acta Crystallogr., Sect. C: Struct. Chem.*, 2015, **71**, 3–8.

